Check for updates

ORIGINAL ARTICLE

Diagnostic Accuracy of Endobronchial Optical Coherence Tomography for the Microscopic Diagnosis of Usual Interstitial Pneumonia

Sreyankar Nandy[1,2,3*], Rebecca A. Raphaely[1,3*], Ashok Muniappan[3,4], Angela Shih[3,5], Benjamin W. Roop[1,2], Amita Sharma[3,6], Colleen M. Keyes[1,3], Thomas V. Colby[7], Hugh G. Auchincloss[3,4], Henning A. Gaissert[3,4], Michael Lanuti[3,4], Christopher R. Morse[3,4], Harald C. Ott[3,4], John C. Wain[3,4,8], Cameron D. Wright[3,4], Maria L. Garcia-Moliner[9], Maxwell L. Smith[7], Paul A. VanderLaan[3,10], Sarita R. Berigei[1,2], Mari Mino-Kenudson[3,5], Nora K. Horick[3,11], Lloyd L. Liang[1], Diane L. Davies[4], Margit V. Szabari[1,2,3], Peter Caravan[3,12,13], Benjamin D. Medoff[1,3] Andrew M. Tager[1,3†], Melissa J. Suter[1,2,3], and Lida P. Hariri[1,2,3,5]

[1]Division of Pulmonary and Critical Care Medicine, [2]Wellman Center for Photomedicine, [4]Division of Thoracic Surgery, [5]Department of Pathology, [6]Department of Radiology, and [11]Biostatistics Center, Massachusetts General Hospital, Boston, Massachusetts; [3]Harvard Medical School, Boston, Massachusetts; [7]Department of Laboratory Medicine and Pathology, Mayo Clinic Arizona, Scottsdale, Arizona; [8]St. Elizabeth's Medical Center, Boston, Massachusetts; [9]Department of Pathology, Rhode Island Hospital and Alpert Medical School, Providence, Rhode Island; [10]Department of Pathology, Beth Israel Deaconess Medical Center, Boston, Massachusetts; [12]Athinoula A. Martinos Center for Biomedical Imaging, Charlestown, Massachusetts; and [13]Institute for Innovation in Imaging (i[3]), Department of Radiology, Massachusetts General Hospital, Charlestown, Massachusetts

ORCID ID: 0000-0002-2553-7109 (S.N.).

Abstract

Rationale: Early, accurate diagnosis of interstitial lung disease (ILD) informs prognosis and therapy, especially in idiopathic pulmonary fibrosis (IPF). Current diagnostic methods are imperfect. High-resolution computed tomography has limited resolution, and surgical lung biopsy (SLB) carries risks of morbidity and mortality. Endobronchial optical coherence tomography (EB-OCT) is a low-risk, bronchoscope-compatible modality that images large lung volumes *in vivo* with microscopic resolution, including subpleural lung, and has the potential to improve the diagnostic accuracy of bronchoscopy for ILD diagnosis.

Objectives: We performed a prospective diagnostic accuracy study of EB-OCT in patients with ILD with a low-confidence diagnosis undergoing SLB. The primary endpoints were EB-OCT sensitivity/specificity for diagnosis of the histopathologic pattern of usual interstitial pneumonia (UIP) and clinical IPF. The secondary endpoint was agreement between EB-OCT and SLB for diagnosis of the ILD fibrosis pattern.

Methods: EB-OCT was performed immediately before SLB. The resulting EB-OCT images and histopathology were interpreted by blinded, independent pathologists. Clinical diagnosis was obtained from the treating pulmonologists after SLB, blinded to EB-OCT.

Measurements and Main Results: We enrolled 31 patients, and 4 were excluded because of inconclusive histopathology or lack of EB-OCT data. Twenty-seven patients were included in the analysis (16 men, average age: 65.0 yr): 12 were diagnosed with UIP and 15 with non-UIP ILD. Average FVC and D_{LCO} were 75.3% (SD, 18.5) and 53.5% (SD, 16.4), respectively. Sensitivity and specificity of EB-OCT was 100% (95% confidence interval, 75.8–100.0%) and 100% (79.6–100%), respectively, for both histopathologic UIP and clinical diagnosis of IPF. There was high agreement between EB-OCT and histopathology for diagnosis of ILD fibrosis pattern (weighted κ: 0.87 [0.72–1.0]).

Conclusions: EB-OCT is a safe, accurate method for microscopic ILD diagnosis, as a complement to high-resolution computed tomography and an alternative to SLB.

Keywords: interstitial lung disease; usual interstitial pneumonia; idiopathic pulmonary fibrosis; *in vivo* optical imaging; *in vivo* microscopy

(Received in original form April 5, 2021; accepted in final form August 10, 2021)

*These authors contributed equally to this work.

†Deceased.

Am J Respir Crit Care Med Vol 204, Iss 10, pp 1164–1179, Nov 15, 2021
Copyright © 2021 by the American Thoracic Society
Originally Published in Press as DOI: 10.1164/rccm.202104-0847OC on August 10, 2021
Internet address: www.atsjournals.org

At a Glance Commentary

Scientific Knowledge on the Subject: Early, accurate diagnosis of interstitial lung disease (ILD) informs prognosis and therapy, but current diagnostic methods are imperfect. High-resolution computed tomography has limited resolution, while surgical lung biopsy (SLB) carries risks of morbidity and mortality. Endobronchial optical coherence tomography (EB-OCT) is a low-risk, bronchoscope-compatible modality that images large lung volumes *in vivo* with microscopic resolution, including subpleural lung, and has potential for ILD diagnosis.

What This Study Adds to the Field: We demonstrate that EB-OCT accurately distinguishes usual interstitial pneumonia (UIP) from non-UIP ILDs, with a sensitivity and specificity of 100% for histopathologic UIP and clinical idiopathic pulmonary fibrosis, and that EB-OCT diagnoses specific fibrotic ILD patterns with a high agreement with corresponding SLB (weighted $\kappa = 0.87$). We also demonstrate that EB-OCT procedural and interpretation skills can easily be acquired by physicians who are unfamiliar with EB-OCT with minimal training. These data support EB-OCT as a low-risk, minimally invasive method for the microscopic diagnosis of ILD, as an adjunct to high-resolution computed tomography and an alternative to SLB.

Interstitial lung disease (ILD) is a heterogeneous group of diseases with variable rates of progression and mortality (1–3). Early, accurate diagnosis of the various ILDs is critical to inform prognosis and guide therapy (2, 3). Idiopathic pulmonary fibrosis (IPF) is progressive and fatal and has a poor prognosis (1). Antifibrotic therapy (e.g., nintedanib, pirfenidone) attenuates the rate of decline in FVC in individuals with IPF and other progressive fibrotic ILDs among patients with restricted and preserved lung function (4–8). For individuals with IPF, antifibrotic therapy is the mainstay of treatment, and immunosuppression is associated with an increased risk of death and hospitalization (2–9). For individuals with non-IPF fibrotic ILDs, however, antifibrotic therapies are often used in conjunction with immune modulating therapy (6). Accordingly, distinguishing between these diagnoses is critical. Furthermore, antifibrotic therapy is not curative, and early intervention is essential to maximize the preservation of lung function (7, 8).

ILD diagnosis requires a multidisciplinary approach including radiographic and/or pathologic assessments (2, 3). IPF is characterized by a usual interstitial pneumonia (UIP) pattern visualized by high-resolution computed tomography (HRCT) and histopathology (2, 3, 10–12). However, HRCT resolution limitations hinder the ability to detect microscopic features, such as honeycombing and traction bronchiectasis <2 mm in diameter, thus precluding a definitive diagnosis in up to 40% of cases, especially in patients with early UIP (2, 3, 12, 13). When HRCT is inconclusive, surgical lung biopsy (SLB) may be indicated for histopathologic diagnosis (2, 3). Unfortunately, SLB carries risk of morbidity and mortality in patients with ILD, with mortality rates averaging 2% for elective procedures (14, 15). These risks mandate a cautious approach to employing SLB for ILD diagnosis and categorically preclude its use in patients with high-risk features. Recently, transbronchial lung cryobiopsy (TBLC) has emerged as a less invasive alternative to SLB, with reported agreement of up to 70.8% (14, 16, 17). However, concerns regarding sampling error, smaller biopsy size, interoperator variability, and risk of pneumothorax and bleeding have limited widespread use (14, 16, 17). Genomic classifiers performed on transbronchial biopsy samples have shown promising results in distinguishing UIP from non-UIP ILD, with a reported sensitivity and specificity of 70% and 88%, respectively, for cases of UIP (18). However, the classifiers are unable to provide information on microscopic features in non-UIP ILD cases.

There is a clear need for low-risk, high-resolution imaging techniques to assist in microscopic ILD diagnosis. Endobronchial optical coherence tomography (EB-OCT) is a minimally invasive, real-time, optical imaging modality that is operated through the working channel of a standard diagnostic bronchoscope and evaluates the peripheral lung without tissue removal (19, 20). EB-OCT uses endogenous tissue contrast to provide *in vivo* three-dimensional imaging in tissue volumes much larger ($\sim 100\times$) than SLB, with microscopic resolution (<10 μm) well beyond HRCT capabilities (19–21). EB-OCT can image many more distinct sites than SLB and can be performed under conscious sedation in a 10- to 15-minute flexible bronchoscopy procedure, obviating the need for mechanical ventilation (20, 22).

Supported in part by the NIH (K23HL132120, R01HL152075, and P41EB015903), Boehringer Ingelheim (BIPI) (Investigator Initiated Study), and the LUNGevity Foundation. BIPI had no role in the design, analysis, or interpretation of the results of this study. BIPI was given the opportunity to review the manuscript for medical and scientific accuracy as it relates to BIPI substances, as well as intellectual property considerations.

Author Contributions: L.P.H. led and S.N., R.A.R., A.M., A. Sharma, P.C., B.D.M., A.M.T., and M.J.S. participated in the study design. A.M., C.M.K., H.G.A., H.A.G., M.L., C.R.M., H.C.O., J.C.W., and C.D.W. performed *in vivo* EB-OCT catheter navigation and data collection. S.N., B.W.R., S.R.B., L.L.L., M.V.S., and L.P.H. assisted with EB-OCT data collection. A. Sharma performed radiology interpretation. L.P.H., M.L.G.M., M.L.S., and P.A.V. performed EB-OCT interpretation. A. Shih, T.V.C., and M.M.-K. performed pathology interpretation. R.A.R. performed clinical follow-up diagnosis evaluation. N.K.H. performed statistical analysis. B.W.R., L.L.L., and D.L.D. conducted patient screening and consenting. S.N., B.W.R., M.J.S., and L.P.H. performed EB-OCT catheter assembly and OCT system maintenance. S.N., R.A.R., B.W.R., S.R.B., N.K.H., and L.P.H. performed data analysis. S.N., R.A.R., and L.P.H. wrote the manuscript, with input from all authors. All authors gave final approval of the manuscript.

Correspondence and requests for reprints should be addressed to Lida P. Hariri, M.D., Ph.D., 55 Fruit Street, Boston, MA 02114. E-mail: lhariri@mgh.harvard.edu.

This article has a related editorial.

Previous *ex vivo* and *in vivo* studies indicate that EB-OCT has the potential to serve as a low-risk method for the evaluation and diagnosis of ILD without tissue removal (20, 22–25). In a pilot study in five patients with ILD undergoing diagnostic SLB for clinical purposes, we preliminarily demonstrated that EB-OCT can detect microscopic features of UIP (20). Here, we conduct a blinded, prospective study to evaluate the diagnostic accuracy of EB-OCT for microscopic ILD diagnosis as compared with concurrent SLB and clinical follow-up diagnosis. Some of the results of these studies have been previously reported in the form of abstracts (26–32).

Methods

Study Design and Subject Enrollment

In this comparative, blinded, prospective, single-center diagnostic accuracy study, inclusion criteria were as follows: *1*) age >21 years, *2*) fibrotic ILD based on HRCT with unclear diagnosis, *3*) SLB required for ILD diagnosis based on the clinical decision of the treating pulmonologist, and *4*) ability to give informed consent. Patients were excluded if their health status precluded participation as determined by the treating physician. Potential subjects were identified from surgical schedules and gave written informed consent to participate in the study. All study-related activities were Health Insurance Portability and Accountability Act of 1996 (HIPAA) compliant, and ethics approval was provided by the Mass General Brigham Institutional Review Board (Protocol #2015P001345).

EB-OCT Imaging and Lung Biopsy Procedure

Subjects underwent EB-OCT during their clinical bronchoscopy, immediately prior to their SLB or TBLC. The bronchoscopist operated the EB-OCT catheter and received a 10-minute standardized training, including how to navigate to and image a sufficient number of lung regions. Study physicians reviewed the most recent HRCT images to identify anatomic subsegmental regions of interest (ROIs) for EB-OCT imaging based on areas of interstitial abnormality. The number of ROIs varied among subjects depending on disease heterogeneity, with a minimum of four ROIs selected per subject.

EB-OCT images were acquired using either an in-house, custom-built OCT system or a commercial OCT system (Ninepoint Medical Nvision), both of which consist of a swept source laser (wavelength, 1,250–1,350 nm) with an axial resolution of 6 μm and penetration depth of up to 3 mm (19–21). A flexible EB-OCT catheter (diameter, 1.65 mm) was advanced through the bronchoscope working channel and extended beyond the visualized region of the bronchoscope until resistance was met in the subpleural lung at each ROI. This method for reaching the subpleural lung was developed and validated in prior *ex vivo* studies of EB-OCT in whole explanted lungs, including lungs with ILD (25). In two subjects, fluoroscopy was performed at the discretion of the bronchoscopist for the clinical biopsy procedure, and the subpleural location of the catheter was visually confirmed in both cases.

Helical cross-sectional images were acquired by rotating the inner optics of the catheter at 12.8 to 66 frames per second. The inner optics of the catheter were retracted with pullback lengths of up to 9 cm (distance over which EB-OCT cross-sectional images were acquired), moving from distal to proximal, generating a three-dimensional helical volume of EB-OCT imaging data. The inner optics were protected by a single-use, sterilized, stationary outer sheath. No moving catheter parts were in contact with tissue during image acquisition. The image-to-image spacing (or pitch) was 33 μm or 50 μm, depending on the system. EB-OCT data were evaluated in real time during the procedure by a pathologist experienced in EB-OCT interpretation and ILD to confirm catheter location in the subpleural lung and ensure adequate image quality and data acquisition for all ROIs.

EB-OCT Data Processing and Interpretation

EB-OCT cross-sectional images were generated from raw data sets and displayed using a grayscale lookup table. Volumetric representations were rendered using 3D Slicer (version 4.11; https://www.slicer.org). EB-OCT criteria (Table 1) were developed from previous *ex vivo* and *in vivo* comparative studies (20, 23–25) for microscopic features of normal and emphysematous parenchyma and histologic fibrotic ILD patterns: UIP, nonspecific interstitial pneumonia (NSIP), and airway-centered fibrosis (ACF) (2, 3, 33).

A pathologist with expertise in ILD and EB-OCT interpretation, referred to as the expert EB-OCT reader, assessed the EB-OCT data from each subject, blinded to histopathology. The expert EB-OCT reader was informed of the anatomic location of each imaging site to assess disease distribution. The expert EB-OCT reader interpreted data from all ROI imaging sites using the criteria in Table 1 to provide a single diagnosis per subject: UIP, NSIP, ACF, mixed ACF/NSIP, or mixed ACF/NSIP/UIP pattern.

Histologic Interpretation

Corresponding lung biopsies were diagnosed by a pathologist with expertise in thoracic pathology at the time of biopsy as part of standard clinical care. A second independent pathologist with expertise in thoracic pathology provided a diagnosis for each subject (deidentified and labeled with a unique study number) at the end of the study. In cases of discrepancy between the two diagnoses, a third independent pathologist with expertise in thoracic pathology provided a diagnosis, and a majority diagnosis was determined. All pathologists arrived at their diagnoses independently and were blinded to EB-OCT results and all prior histology interpretation. All pathologists had experience in ILD and used established criteria for the histopathologic diagnosis of UIP pattern as specified by the 2011 and 2018 American Thoracic Society (ATS)/European Respiratory Society/Japanese Respiratory Society/Latin American Thoracic Society Clinical Practice Guidelines and the 2018 Fleischer Society Guidelines for the diagnosis of UIP/IPF (2, 3, 33). The criteria for the diagnosis of a histopathologic UIP pattern is consistent across the guidelines, and there were no significant changes in the ATS guidelines between 2011 and 2018 (2, 3, 33).

Clinical Follow-up Diagnosis

Each treating pulmonologist conducted a systematic review of the clinical, HRCT, SLB, and serology data to determine a clinical follow-up diagnosis for each patient as a part of clinical care. A multidisciplinary discussion (MDD) conference was conducted if deemed necessary. A separate, independent pulmonologist reviewed all data to confirm clinical follow-up diagnoses. All pulmonologists were blinded to EB-OCT.

Table 1. EB-OCT Imaging Features of Interstitial Lung Disease

Microscopic Feature	EB-OCT Imaging Feature
Normal lung parenchyma	Regions of evenly spaced, small (150–500 μm), lattice-like, signal-void (black) alveoli separated by thin, gray alveolar walls, attached to the bronchiolar wall (Figure 2).
Emphysema	Enlarged (1.5–4.5 mm), irregular-shaped, signal-void (black) alveolar airspaces, with thin, gray alveolar walls showing evidence of fragmentation. Minimal to no fibrosis is present (Figure 5).
Usual interstitial pneumonia	
Destructive subpleural fibrosis	Dense, homogeneous, signal-intense (gray to light gray) subpleural tissue replacing normal, lattice-like, signal-void (black) alveoli (Figures 3 and 4).
Microscopic honeycombing	Irregularly shaped, signal-poor (black to dark gray), clustered, dilated cystic structures (0.5–3 mm), with mildly thickened, signal-moderate (gray) walls, embedded within dense, signal-intense (gray to light gray) fibrosis. Cystic structures do not connect to the main airway, distinguishing them from traction bronchiectasis (Figures 3 and 4).
Traction bronchiectasis	Cystic, dilated, and/or distorted, signal-void (black) airway branch points that connect to the main airway, associated with signal-intense (gray to light gray) fibrosis. May be present but is not required or specific for usual interstitial pneumonia (Figure 4).
Spatial heterogeneity	Regions of preserved alveolar, signal-void (black) parenchyma adjacent to regions of destructive, signal-intense (gray to light gray) fibrosis. May appear normal or with interstitial fibrosis in a nonuniform nonspecific interstitial pneumonia–like pattern (Figure 2).
Absence of features indicating alternative diagnosis	Absence of conspicuous airway-centered fibrosis.
Nonspecific interstitial pneumonia	
Nondestructive interstitial fibrosis	Evenly spaced signal-void (black) alveoli with mild, uniform signal-intense (gray to light gray) thickening of alveolar walls, present homogeneously throughout the parenchyma (Figure 6).
Mild traction bronchiectasis	May be seen but is not required.
Airway-centered fibrosis	
Fibrosis centered on airway	Dense, signal-intense (gray to light gray) fibrosis around airways, with preserved alveolar architecture distal to the region of fibrosis. Fibrosis may be either destructive or nondestructive of attached signal-void (black) alveoli (Figure 7).
Traction bronchiectasis	Frequently seen, often involving more proximal airway branch points (Figure 7).
Peribronchiolar metaplasia	May be seen. Appears as small-sized, irregular, signal-poor (black to dark gray) cystic structures immediately adjacent to proximal traction bronchiectasis (Figure 7).
Hyperinflation	May be seen. Appears as enlarged, rounded, signal-void (black) alveolar airspaces, with intact gray alveolar walls (Figure 7).

Definition of abbreviation: EB-OCT = endobronchial optical coherence tomography.

Training and Testing of Novice EB-OCT Readers

To evaluate the ability of pathologists to learn to interpret EB-OCT images, three board-certified pathologists with expertise in ILD and no prior experience with OCT imaging (referred to as novice readers) were trained and tested on EB-OCT interpretation. After completion of the initial study analysis by the expert EB-OCT reader, the study data were divided into training and testing data sets, with each data set comprising 50% of the study subjects, with equal proportions of each ILD diagnosis. The novice pathologist readers participated in a 3-hour training session with the expert EB-OCT reader, which covered the basic principles of EB-OCT and the application of EB-OCT imaging criteria for the diagnosis of UIP and non-UIP ILD using subject cases from the training data set. Following the training

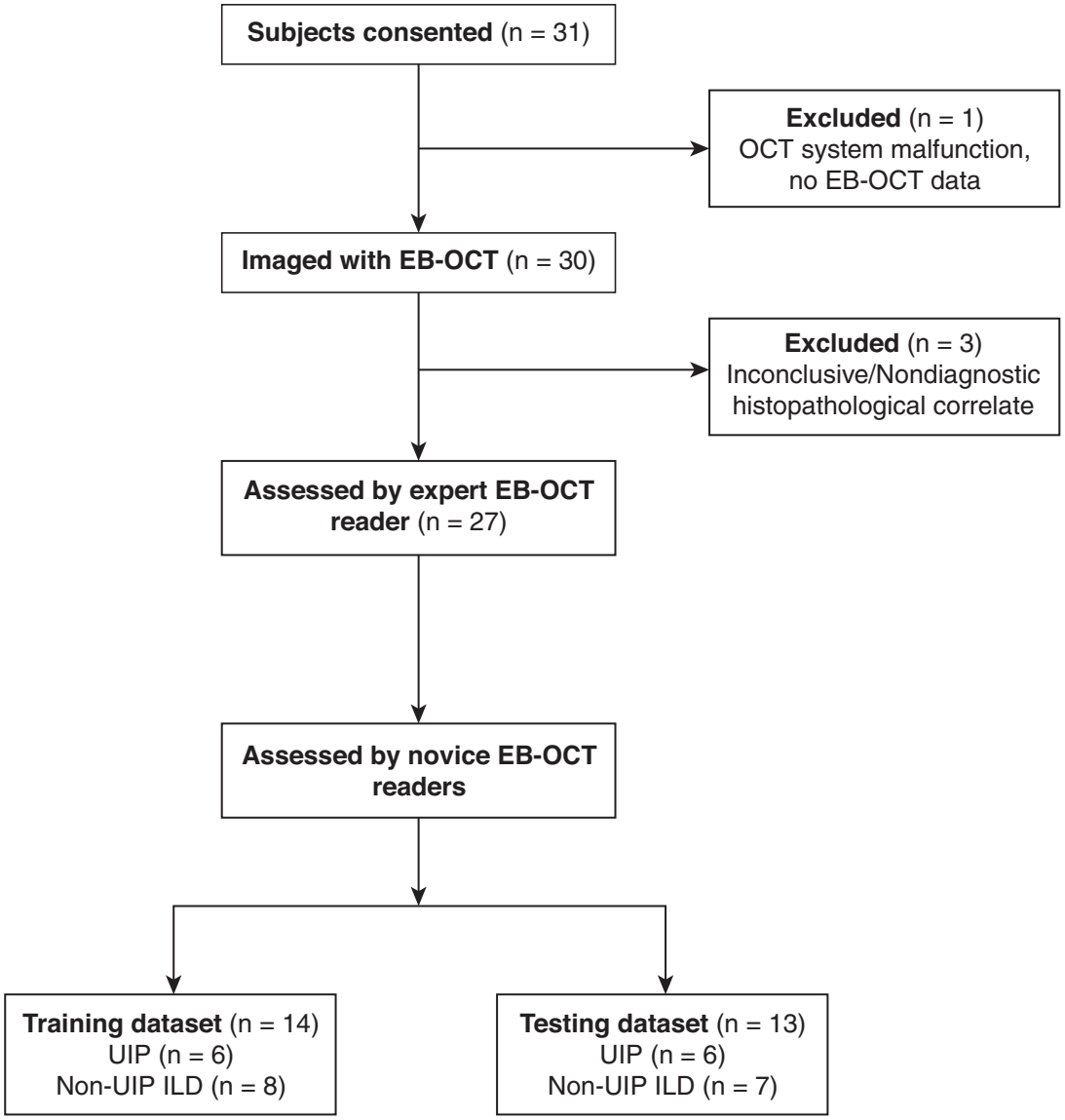

Figure 1. Flow diagram of study enrollment. EB-OCT = endobronchial optical coherence tomography; ILD = interstitial lung disease; UIP = usual interstitial pneumonia.

session, the novice pathologist readers were asked to independently evaluate the EB-OCT data for each subject in the testing data set, blinded to histopathology and the assessment of the EB-OCT data by the expert reader. The readers were informed of the anatomic location of each imaging site to assess disease distribution. Novice readers were asked to interpret data from all ROI imaging sites using the criteria in Table 1 to provide a single diagnosis per subject of either UIP or non-UIP ILD pattern.

Statistical Analysis

Based on UIP prevalence of 50%, in accordance with data from our ILD center, a sample size of 24 subjects would enable an estimation of sensitivity and specificity of at least 90% for UIP, with 89% power and a lower 95% confidence limit of at least 0.5 (34).

Primary endpoints were sensitivity and specificity of EB-OCT for the diagnosis of UIP and IPF, as compared to independently evaluated histopathological diagnosis and clinical follow-up diagnosis, respectively. UIP was defined as EB-OCT or histopathology with pure UIP, without mixed ACF pattern. Gwet's AC1 statistic was used to assess interrater reliability among the novice EB-OCT pathologist readers. The secondary endpoint for the expert EB-OCT reader was the agreement between the specific fibrotic ILD pattern diagnosis based on EB-OCT and that based on histopathology, and ordinal categorical diagnoses were compared with unweighted and Cicchetti–Allison weighted Cohen's κ statistic. All statistical analyses are presented with 95% confidence intervals (95% CIs). All analyses were performed using SAS software (version 9.4).

Results

Study Subject Cohort

Between November 2015 and March 2020, 31 patients with a low-confidence diagnosis

Table 2. Baseline Patient Demographics and Characteristics for the EB-OCT Study Cohort

	Value
Sex	
M	16 (59)
F	11 (41)
Age, yr	65.0 ± 8.0
Body mass index, kg/m^2	30.0 ± 5.8
Smoking status	
Never	6 (22)
Former	21 (78)
Current	0 (0)
Pack-years (former smokers)	21.2 ± 20.7
Lung function measurements (all subjects, $n = 25$)	
FVC, % of predicted value	75.3 ± 18.5
D_{LCO}, % of predicted value	53.5 ± 16.4
Lung function measurements (subjects with UIP/IPF)	
FVC, % of predicted value	83.9 ± 16.8
D_{LCO}, % of predicted value	60.4 ± 13.1
Lung function measurements (subjects without UIP/IPF)	
FVC, % of predicted value	68.0 ± 17.2
D_{LCO}, % of predicted value	45.1 ± 16.5

Definition of abbreviations: EB-OCT = endobronchial optical coherence tomography; ILD = interstitial lung disease; IPF = idiopathic pulmonary fibrosis; UIP = usual interstitial pneumonia.
Data are shown as *n* (%) or mean ± SD, unless otherwise stated. There is a statistically significant difference ($P < 0.05$) for comparisons of both FVC and D_{LCO} (% predicted value) between UIP and non-UIP ILD.

or unclassifiable ILD were enrolled in the study. Four patients were excluded (Figure 1): three due to inconclusive/nondiagnostic biopsies and one due to a lack of EB-OCT data owing to a minor system malfunction prior to the study imaging procedure. Of the three inconclusive/nondiagnostic cases, two had lower lobe predominant disease as assessed by HRCT but underwent upper 3lobectomy for resection of a lung nodule that was concerning for malignancy, and middle/lower lobe biopsies were not obtained owing to patient safety concerns. The third case was a patient with a nondiagnostic TBLC specimen who declined subsequent SLB. The remaining 27 subjects were included in the analysis (Figure 1): 16 (59%) men and 11 (41%) women with a mean age of 65.0 years (SD, 8.0). Of the 27 subjects, 16 (59%) were presented in MDD conference by their treating pulmonologist. Baseline patient characteristics are shown in Table 2.

Patients generally had mild to moderate impairment on lung function tests, with an average percent-predicted FVC of 75.3% (SD, 18.5) and an average D_{LCO} of 53.5% (SD, 16.4). Patients who received a diagnosis of UIP on SLB and IPF on clinical follow-up had higher FVC and D_{LCO} values than the patients with non-UIP/IPF ILD (Table 2). Twenty-four patients underwent SLB, and three underwent TBLC. Only one TBLC was diagnostic. The two patients for whom TBLC was nondiagnostic underwent SLB 2 to 3 months later, which was used as the EB-OCT histologic comparator.

EB-OCT Imaging Procedure

Nine physicians (eight thoracic surgeons and one interventional pulmonologist) experienced in bronchoscopy underwent training on EB-OCT imaging and successfully performed EB-OCT. Of the nine physicians, seven had no prior experience with OCT imaging and two (one thoracic surgeon and one interventional pulmonologist) had previously performed EB-OCT in patients with lung cancer with central airway masses (fewer than 5 cases each). There were no adverse events associated with the EB-OCT imaging procedure. The average bronchoscopy time for EB-OCT was 9.5 minutes (SD, 4.22). Volumetric EB-OCT was obtained from multiple locations in the upper, middle, and lower lung lobes (average, 6 EB-OCT ROI imaging sites per patient; range, 1–9 sites), with up to 8.7-cm-long pullback lengths per ROI (average, 4 cm; SD, 1.5 cm). Each ROI imaging site generated an average of 1,340 cross-sectional images, which were all assessed for diagnosis. In two patients, only one EB-OCT ROI was acquired because of time constraints from a prolonged diagnostic bronchoscopy prior to EB-OCT or EB-OCT catheter malfunction after the first ROI. In both cases, interpretable EB-OCT data were still obtained. In the remaining 25 patients, at least four EB-OCT ROIs were acquired.

Histopathology and Clinical Follow-up Diagnosis

On histopathology, 12 patients received a diagnosis of UIP (44.5%) and 15 received a diagnosis of non-UIP (55.5%): 3 as mixed UIP/ACF/NSIP (11.1%), 1 as ACF (3.7%), 7 as mixed ACF/NSIP (25.9%), 3 as NSIP (11.1%), and 1 as other (diffuse idiopathic pulmonary neuroendocrine cell hyperplasia with carcinoid tumorlets) (3.7%). In 19 cases (70.4%), two independent pathologists agreed on the diagnoses. In the remaining eight cases (29.6%), a third independent pathologist provided a diagnosis, and a majority diagnosis was rendered. All patients who received a diagnosis of histologic UIP pattern were classified as having clinical IPF by the treating pulmonologist.

Expert EB-OCT Reader Analysis

In the expert EB-OCT reader analysis, EB-OCT diagnosis of UIP achieved a sensitivity of 100% (95% CI, 75.8–100%) and a specificity of 100% (79.6–100%) as compared with the histopathologic diagnosis of UIP and the clinical follow-up diagnosis of IPF. The positive predictive value (PPV) and negative predictive value (NPV) were both 100% for UIP and IPF, respectively. The raw agreement between paired EB-OCT and

Table 3. EB-OCT Diagnosis as Compared Independently with Histologic Diagnosis and Clinical Follow-up Diagnosis

EB-OCT Diagnosis	Histopathology Diagnosis	Clinical Follow-up Diagnosis
UIP	UIP	IPF
Mixed NSIP + ACF	Mixed NSIP and ACF	Likely FHP, but no antigen source identified
UIP	UIP	IPF (limited scleroderma likely unrelated to UIP)
UIP	UIP	IPF
UIP	UIP	IPF
UIP	UIP	IPF
UIP	UIP	IPF
Mixed ACF + NSIP	Mixed ACF + NSIP	FHP
Mixed ACF + NSIP	Mixed ACF + NSIP	CTD-ILD (myositis)
Mixed NSIP + ACF	NSIP + ACF	Likely FHP, but no antigen source identified
UIP	UIP	IPF
Mixed ACF + NSIP	Mixed ACF + NSIP	Likely FHP, but no antigen source identified
Mixed ACF + NSIP + UIP	Mixed ACF + NSIP + UIP	Fibrotic ILD of unclear etiology, possibly from inhalational exposure. Not IPF
UIP	UIP	IPF
Mixed NSIP + ACF + UIP	NSIP	FHP (bird exposure)
UIP	UIP	IPF
UIP	UIP	IPF
NSIP	NSIP	Idiopathic fibrotic NSIP
UIP	UIP	IPF
Mixed ACF + NSIP + UIP	Mixed ACF + NSIP + UIP	Likely FHP, but no antigen source identified
Mixed ACF + NSIP	NSIP	CTD-ILD (SLE)
Mixed ACF + NSIP + UIP	Mixed ACF + NSIP +UIP	Fibrotic ILD of unclear etiology, possibly from inhalational exposure. Not IPF
ACF	ACF	Fibrotic ILD of unclear etiology, possibly from inhalational exposure. Not IPF
Mixed ACF + NSIP	Mixed ACF + NSIP	Autoimmune-related ILD (IBD)
Mild ACF + NSIP; small mass lesion in LLL	Other (DIPNECH with carcinoid tumorlets)	DIPNECH
UIP	UIP	IPF
Mixed ACF + NSIP	Mixed ACF + NSIP	CTD-ILD (myositis)

Definition of abbreviations: ACF = airway-centered fibrosis; CTD-ILD = connective tissue disease–related interstitial lung disease; DIPNECH = diffuse idiopathic pulmonary neuroendocrine cell hyperplasia; EB-OCT = endobronchial optical coherence tomography; FHP = fibrotic hypersensitivity pneumonitis; IBD = inflammatory bowel disease; IPF = idiopathic pulmonary fibrosis; LLL = left lower lobe; NSIP = nonspecific interstitial pneumonia; SLE = systemic lupus erythematosus; UIP = usual interstitial pneumonia.

Table 4. EB-OCT Sensitivity and Specificity for Histopathologic UIP and Clinical IPF for Expert and Novice EB-OCT Readers

EB-OCT Reader	No. of Cases	Sensitivity (95% CI) (%)	Specificity (95% CI) (%)	PPV (95% CI) (%)	NPV (95% CI) (%)
Expert EB-OCT reader	27 (12 UIP/15 non-UIP ILD)	100 (75.8–100)	100 (79.6–100)	100 (73.5–100)	100 (78.2–100)
Novice EB-OCT reader 1	13 (6 UIP/7 non-UIP ILD)	100 (54.1–100)	100 (59.0–100)	100 (54.1–100)	100 (59.0–100)
Novice EB-OCT reader 2	13 (6 UIP/7 non-UIP ILD)	100 (54.1–100)	100 (59.0–100)	100 (54.1–100)	100 (59.0–100)
Novice EB-OCT reader 3	13 (6 UIP/7 non-UIP ILD)	66.7 (22.3–95.7)	100 (59.0–100)	100 (39.8–100)	77.8 (40.0–97.2)

Definition of abbreviations: CI = confidence interval; EB-OCT = endobronchial optical coherence tomography; ILD = interstitial lung disease; IPF = idiopathic pulmonary fibrosis; NPV = negative predictive value; PPV = positive predictive value; UIP = usual interstitial pneumonia.
All cases of histopathologic UIP on lung biopsy were determined to be clinical IPF.

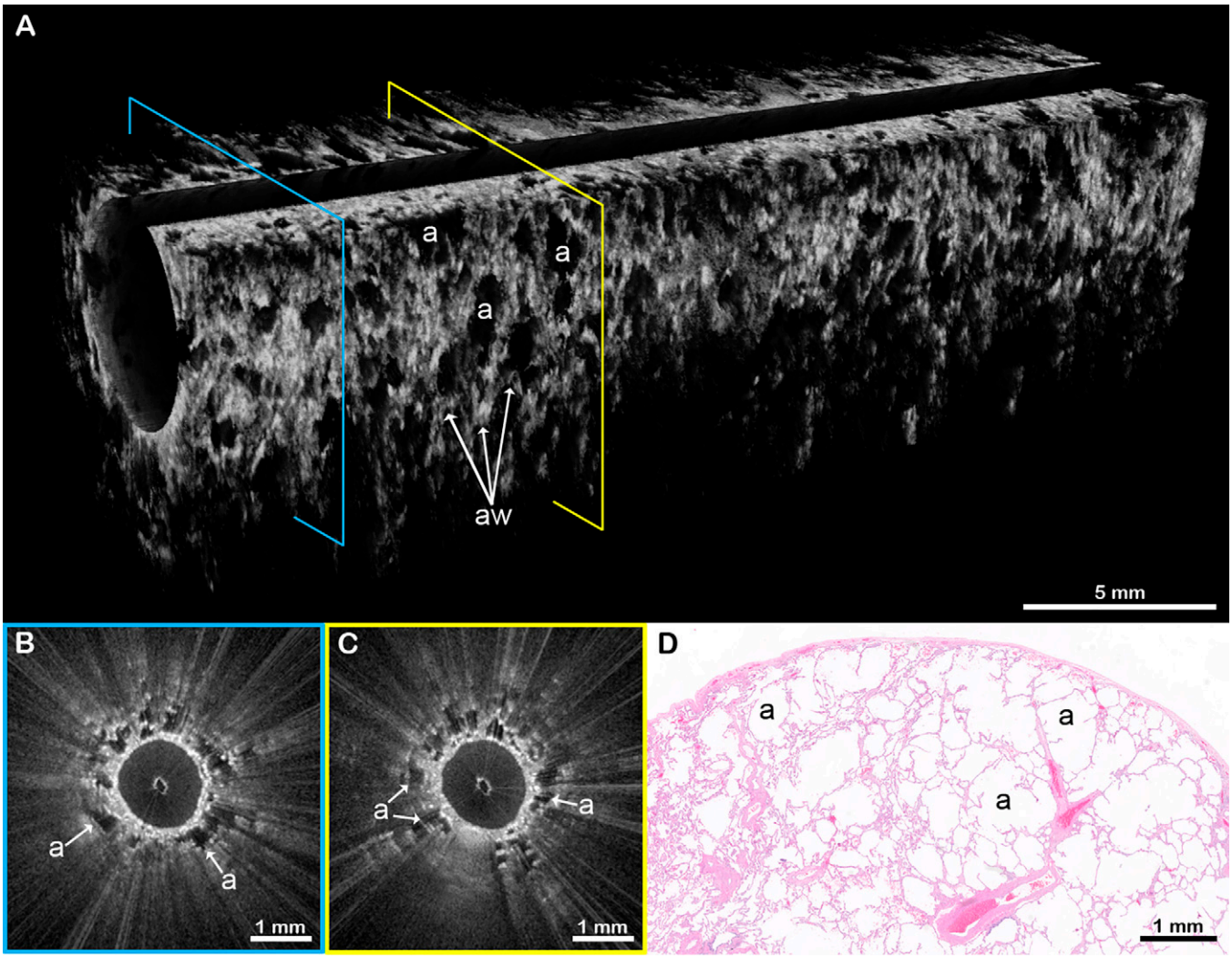

Figure 2. EB-OCT of alveolar lung parenchyma. (*A*) *In vivo* volumetric EB-OCT and (*B* and *C*) corresponding cross-sectional EB-OCT images from the upper lobe show alveolated lung parenchyma with minimal fibrosis. Alveoli appear as round, evenly spaced and sized, signal-void (black) structures with thin, lattice-like alveolar walls attached to the thin distal bronchiolar wall. (*D*) Representative histology from the surgical lung biopsy confirms regions of preserved lung parenchyma with minimal interstitial fibrosis. The EB-OCT cross-sections in *B* and *C* are taken from the locations on the volumetric image (*A*) indicated by the blue and yellow squares, respectively. a = alveoli; aw = alveolar walls; EB-OCT = endobronchial optical coherence tomography.

histopathologic diagnosis of specific ILD fibrosis patterns was 84.0% (95% CI, 66.7–100.0%), with a Cicchetti-Allison weighted κ of 0.87 (95% CI, 0.72–1.0) and an unweighted κ of 0.84 (95% CI, 0.68–1.0). EB-OCT image interpretation by the expert reader, histopathology diagnosis, and clinical follow-up diagnosis for all subjects are presented in Table 3.

Novice EB-OCT Reader Analysis

In the novice EB-OCT pathologist reader analysis (Table 4), two readers achieved a sensitivity of 100% (95% CI, 54.1–100%) and a specificity of 100% (95% CI, 59.0–100%) for the histopathologic diagnosis of UIP and the clinical follow-up diagnosis of IPF. The PPV and NPV in comparison with histopathologic diagnosis and clinical follow-up were both 100% for UIP and IPF, respectively. The third novice pathologist reader achieved a sensitivity of 66.7% (95% CI, 22.3–95.7%) and a specificity of 100% (95% CI, 59.0–100%) as compared with the histopathologic diagnosis of UIP and the clinical follow-up diagnosis of IPF. The PPV was 100% and the NPV was 77.8% in comparison with histopathologic diagnosis of UIP and clinical follow-up diagnosis of IPF. Interrater reliability for the three novice EB-OCT pathologist readers was 0.80 ($P < 0.0001$), indicating strong agreement among the novice readers.

EB-OCT Case Examples

Example EB-OCT images from the spectrum of fibrotic ILD patterns are presented in Figures 2–7. Figures 2 and 3 are from a 64-year-old man who received a diagnosis of IPF. EB-OCT visualized intact alveolar lung parenchyma in the upper lobe (Figure 2) and UIP features in the lower lobe (Figure 3). On subsequent SLB, there was dense, destructive, subpleural fibrosis with infrequent cystic structures, consistent with microscopic

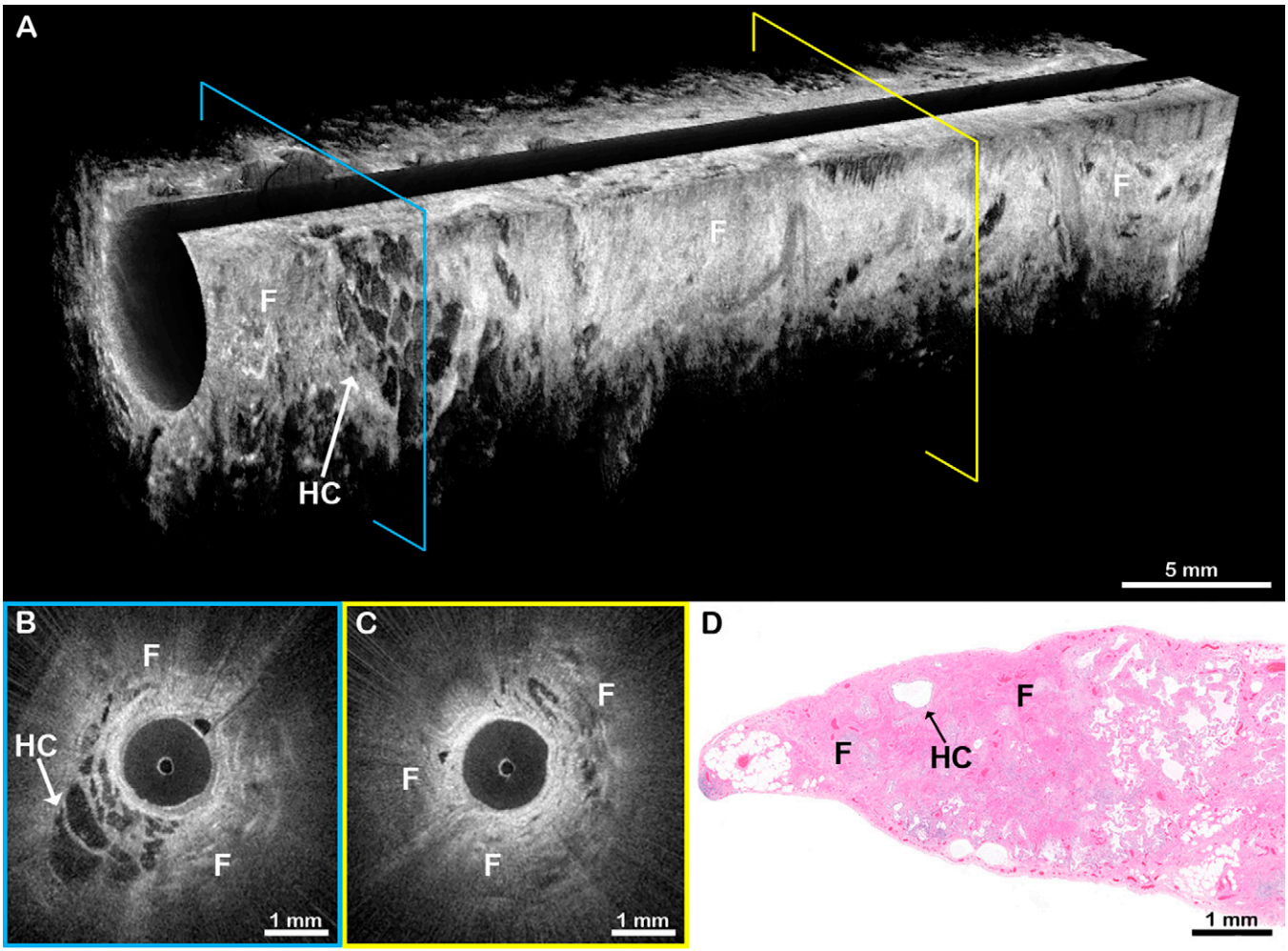

Figure 3. EB-OCT of UIP in a patient ultimately diagnosed with histopathologic UIP and clinical IPF. (*A*) *In vivo* volumetric EB-OCT and (*B* and *C*) corresponding cross-sectional EB-OCT images from the lower lobe of the same patient in Figure 2 show features of UIP. Dense, signal-intense (light gray to white) subpleural fibrosis has obliterated alveolar structures. Embedded within the fibrosis are clusters of enlarged, irregularly shaped, stacked, signal-poor (black to dark gray) cystic structures, consistent with microscopic honeycombing. (*D*) Subsequent surgical lung biopsy confirms dense, destructive subpleural fibrosis with infrequent, individual cystic honeycomb-like structures. The consensus histopathologic diagnosis was UIP, but there was wide discrepancy among the reviewing pathologists, owing primarily to the absence of honeycombing. The diagnosis of UIP was ultimately confirmed 3 years later on surgical explant lung histology at the time of lung transplantation, and the patient was clinically diagnosed with IPF. The EB-OCT cross-sections in *B* and *C* are taken from the locations on the volumetric image (*A*) indicated by the blue and yellow squares, respectively. EB-OCT = endobronchial optical coherence tomography; F = fibrosis; HC = microscopic honeycombing; IPF = idiopathic pulmonary fibrosis; UIP = usual interstitial pneumonia.

honeycombing (Figure 3D). The histopathologic majority diagnosis was UIP, but there was wide discrepancy among the reviewing pathologists primarily due to the sparsity of honeycombing. Three years later, a diagnosis of UIP was made on surgical explant lung histology at the time of lung transplantation, and, subsequently, the patient was clinically diagnosed with IPF.

In an example of combined pulmonary fibrosis with emphysema from a 77-year-old man (Figures 4 and 5), EB-OCT from the basilar segment of the lower lobe visualized UIP features (Figure 4). EB-OCT from the upper lobe and the superior segment of the lower lobe (Figure 5) showed alveolated lung parenchyma with enlarged alveolar spaces and fragmented alveolar walls, consistent with emphysema. SLB confirmed the diagnoses of UIP and emphysema, and the clinical follow-up diagnosis was IPF in a patient with combined pulmonary fibrosis with emphysema.

NSIP is a fibrotic ILD pattern that can be seen idiopathically or in the setting of fibrotic hypersensitivity pneumonitis (FHP) or connective tissue disease related ILD (CTD-ILD). EB-OCT images from a 65-year-old woman showed features of NSIP (Figure 6) with preserved alveolar architecture and mild, homogeneous fibrotic thickening of interstitial alveolar walls. SLB confirmed the diagnosis of NSIP.

ACF is a fibrotic ILD pattern that can be seen in FHP, CTD-ILD, and aspiration,

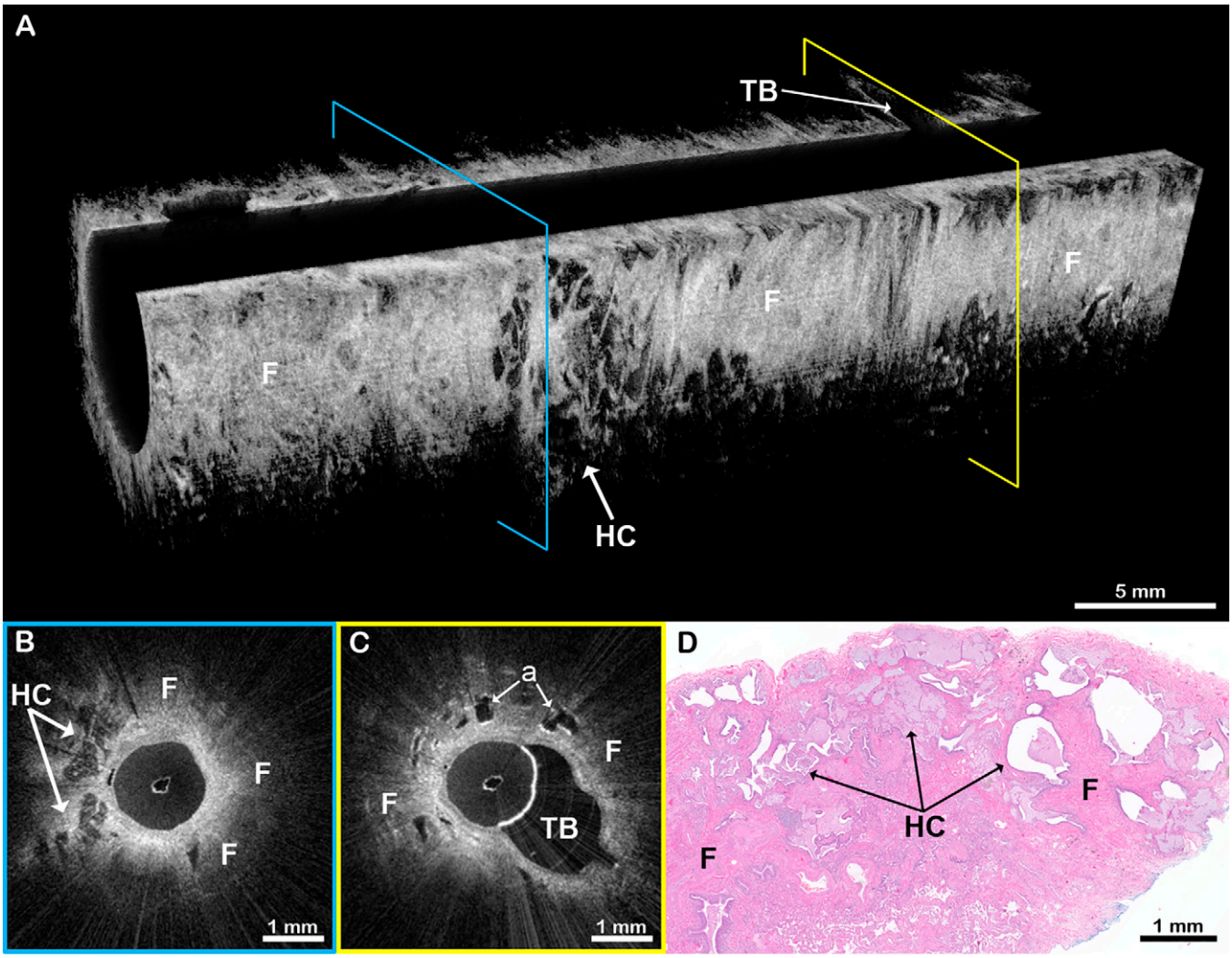

Figure 4. EB-OCT of UIP in a patient with combined pulmonary fibrosis and emphysema. (*A*) *In vivo* volumetric and (*B* and *C*) cross-sectional EB-OCT images from the basilar segment of the lower lobe show features of UIP, including microscopic honeycombing embedded in a background of dense, destructive subpleural fibrosis. A region of traction bronchiectasis can be seen as an abnormally dilated, tortuous airway branch point with fibrosis and some adjacent preserved alveolar spaces. (*D*) Corresponding surgical lung biopsy shows dense destructive fibrosis with microscopic honeycombing. The clinical follow-up diagnosis was idiopathic pulmonary fibrosis with emphysema, also known as combined pulmonary fibrosis and emphysema. The EB-OCT cross-sections in *B* and *C* are taken from the locations on the volumetric image (*A*) indicated by the blue and yellow squares, respectively. a = preserved alveolar spaces; EB-OCT = endobronchial optical coherence tomography; F = fibrosis; HC = microscopic honeycombing; TB = traction bronchiectasis; UIP = usual interstitial pneumonia.

either as pure ACF or mixed with regions of UIP pattern. Typically, the presence of conspicuous ACF on histology argues against a diagnosis of IPF. Figure 7 illustrates an example of ACF in a 69-year-old woman. EB-OCT showed fibrosis surrounding the proximal end of the airway with traction bronchiectasis and associated peribronchiolar metaplasia. There is a transition distally to alveolated parenchyma, with enlarged, rounded airspaces and intact alveolar walls, indicative of hyperinflation. SLB confirmed the diagnosis of ACF ILD.

Discussion

Early, accurate diagnosis of ILD is critical for clinical management, prognostication, and therapeutic decision-making. The current standard diagnostic methods have limited resolution or carry risks of morbidity and mortality (2, 3, 12–17). Here, we demonstrate that EB-OCT accurately distinguishes UIP from non-UIP ILDs, with a sensitivity and specificity of 100% for histopathologic UIP and clinical IPF, and that EB-OCT diagnoses specific fibrotic ILD patterns with a high agreement with corresponding SLB (weighted $\kappa = 0.87$). We also demonstrate that EB-OCT procedural and interpretation skills can easily be acquired with minimal training by physicians who are unfamiliar with EB-OCT. We successfully trained nine bronchoscopists to obtain adequate EB-OCT data in $<$10 minutes per patient and trained three pathologists to interpret EB-OCT data, with two pathologists achieving a sensitivity and specificity of 100% for histopathologic UIP and clinical

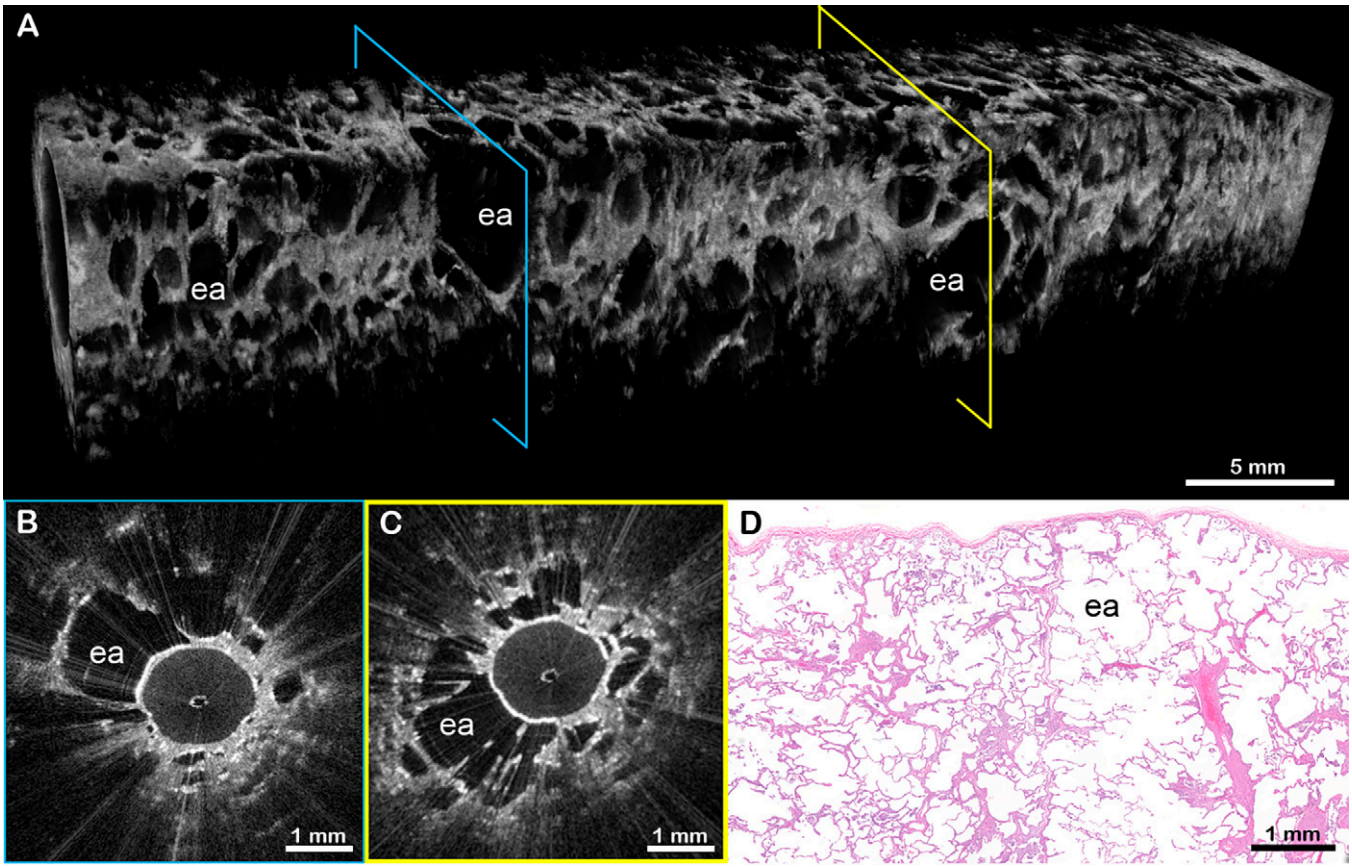

Figure 5. EB-OCT of emphysema in a patient with combined pulmonary fibrosis and emphysema. (*A*) *In vivo* volumetric and (*B* and *C*) cross-sectional EB-OCT images from the superior segment of the lower lobe in the same patient as Figure 4 show emphysema, demonstrated as irregularly shaped, abnormally enlarged airspaces with focal destruction of alveolar walls. Fibrosis was minimal. (*D*) Corresponding surgical lung biopsy confirms the presence of emphysema. The emphysematous changes are distinguishable from usual interstitial pneumonia seen in the patient's lower lobe basilar segment (Figure 4). The clinical follow-up diagnosis was idiopathic pulmonary fibrosis with emphysema, also known as combined pulmonary fibrosis and emphysema. The EB-OCT cross-sections in *B* and *C* are taken from the locations on the volumetric image (*A*) indicated by the blue and yellow squares, respectively. CPFE = combined pulmonary fibrosis and emphysema; ea = enlarged airspaces; EB-OCT = endobronchial optical coherence tomography.

IPF. These data support EB-OCT as a low-risk, minimally invasive method for the microscopic diagnosis of ILD, as an adjunct to HRCT and an alternative to SLB (Figure 8), that has the potential for widespread use.

The ability to accurately diagnose and subtype ILD—especially IPF—at early disease stages is paramount to optimizing treatment. The INBUILD trial demonstrated that antifibrotic therapy, nintedanib, preserves lung function in individuals with UIP and those with other progressive fibrotic ILDs. However, the use of concurrent immunosuppressive therapy should be limited to patients with non-IPF ILD (6, 9). Additionally, studies have shown that antifibrotic therapies slow the rate of FVC decline in patients with UIP/IPF with preserved lung function (7, 8). Therefore, it is anticipated that antifibrotic therapy initiated at early disease stages will have further protective effects against pulmonary function decline and will, therefore, have further clinical benefits for patients. This requires a diagnosis in the early disease stages, when features distinguishing the different types of fibrotic ILDs may not be identifiable on HRCT (10–13). In this study, participants with UIP had relatively preserved lung function without macroscopic honeycomb cysts on HRCT, demonstrating that EB-OCT may be useful for diagnosing early ILD with minimal risk.

EB-OCT is inherently safer than SLB and TBLC, because no tissue removal is required (14–17). There were no adverse events associated with EB-OCT use in this study. Previously, we have shown that EB-OCT can be safely performed during a 10- to 15-minute flexible bronchoscopy under conscious sedation (22). This removes the requirement for mechanical ventilation or general anesthesia that contributes to the risks of morbidity associated with SLB in patients with ILD. Here, we conducted EB-OCT in an average of 9.5 minutes per patient, including intraprocedural EB-OCT adequacy evaluation and time for occasional instances requiring catheter repositioning. This is significantly less time than is needed for standard SLB procedures and, accordingly, reduces the risk to the patient.

Although our study represents data from a single center, our results indicate that other physicians can easily be trained to acquire and interpret EB-OCT data, thus suggesting that this technique could be readily expanded to other sites. In the TBLC literature, interoperator variability has been identified as a potential cause of variable

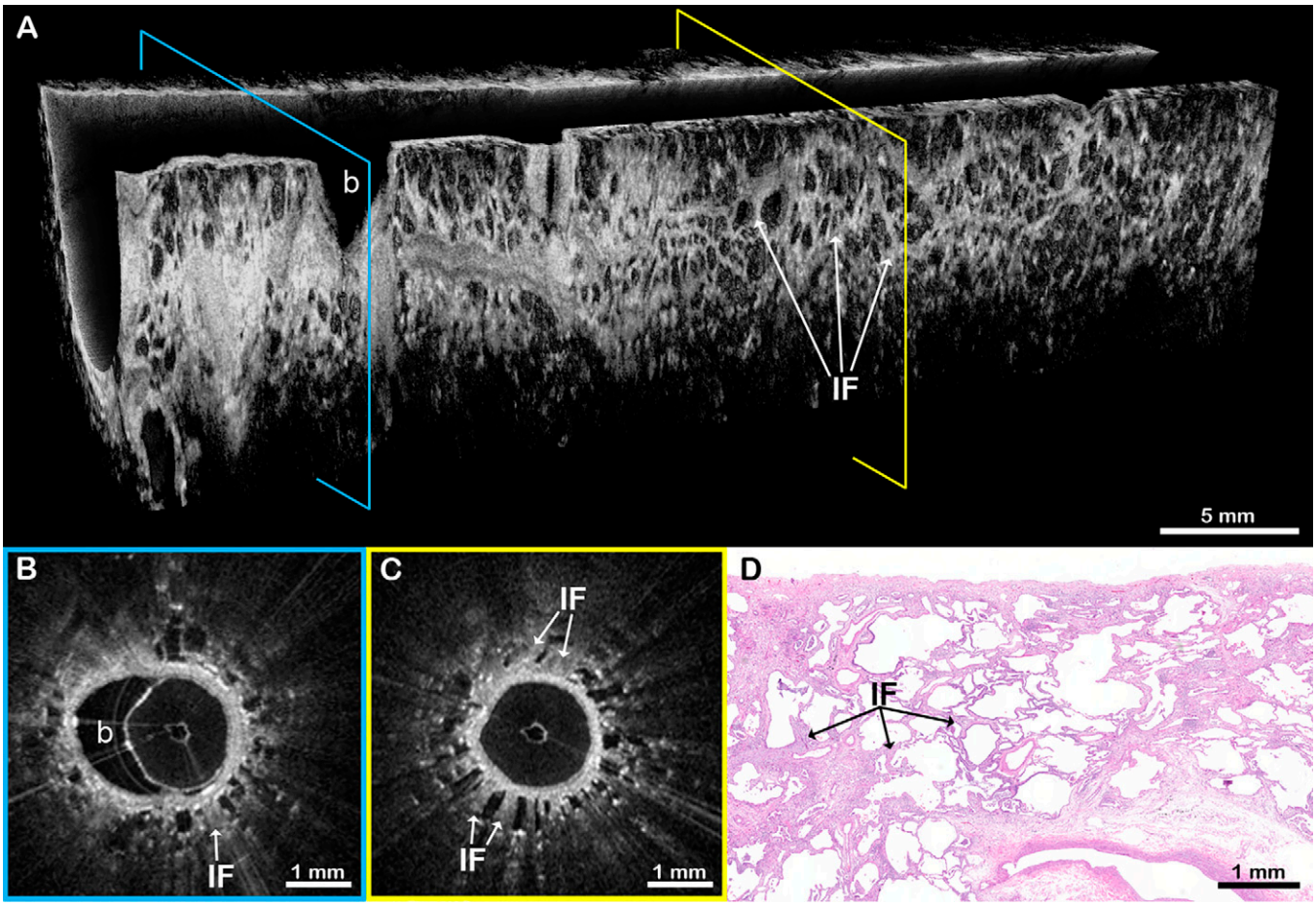

Figure 6. EB-OCT in a patient with NSIP. (*A*) *In vivo* volumetric and (*B* and *C*) cross-sectional EB-OCT images show preserved alveolar architecture with mild, homogeneous fibrotic thickening of the interstitial alveolar walls, consistent with NSIP. A small normal bronchiolar airway branch point can also be seen. (*D*) Subsequent surgical lung biopsy confirms homogeneous interstitial fibrosis and the diagnosis of NSIP. The EB-OCT cross-sections in *B* and *C* are taken from the locations on the volumetric image (*A*) indicated by the blue and yellow squares, respectively. b = bronchiolar airway branch point; EB-OCT = endobronchial optical coherence tomography; IF = interstitial fibrosis in alveolar walls; NSIP = nonspecific interstitial pneumonia.

rates in diagnostic accuracy and adverse events (14, 16, 17). Here, we found that a 10-minute training in EB-OCT imaging acquisition was sufficient for nine physicians, who had little to no prior experience with OCT imaging, to collect interpretable data for all patients. The ease of performing EB-OCT will aid in standardizing the procedure for future multicenter use. Although the study initially used one expert EB-OCT reader, because of the need for expertise in both ILD and EB-OCT, we demonstrated that pathologists without prior experience with OCT can successfully interpret EB-OCT images after a 3-hour training session. In our study, two of the novice EB-OCT readers achieved a sensitivity and specificity of 100% for histopathologic UIP and clinical IPF. Although a third novice EB-OCT reader achieved a lower sensitivity (66.7%), specificity was still 100% for histopathologic UIP and clinical IPF. We anticipate that additional training and experience with EB-OCT would likely improve interpretation skills. The study sample size was not sufficient to allow for adequate training and testing of the novice pathologist readers on specific fibrotic ILD patterns within the non-UIP ILD category. However, because the EB-OCT imaging features are direct correlates of histopathologic features, we do not anticipate difficulty in training ILD pathology experts to identify specific fibrotic ILD patterns, and we will evaluate this in future, larger-scale studies.

EB-OCT imaging data are presented in real time. This feature allows for the intraprocedural assessment of EB-OCT images, helping to ensure that sufficient data are obtained for diagnosis and avoid the need for repeat or more invasive procedures. In this study, a pathologist with expertise in ILD and EB-OCT interpretation was present during the procedure to confirm subpleural positioning of the EB-OCT catheter at the beginning of each scan and to ensure adequate data quality and sampling of anatomic sites for diagnosis. We anticipate that pathologists trained in EB-OCT interpretation—such as the novice EB-OCT readers trained in this study—may provide intraprocedural consultation on imaging quality and adequacy, similar to frozen section evaluation of SLB. Moreover, we have previously shown that pulmonologists

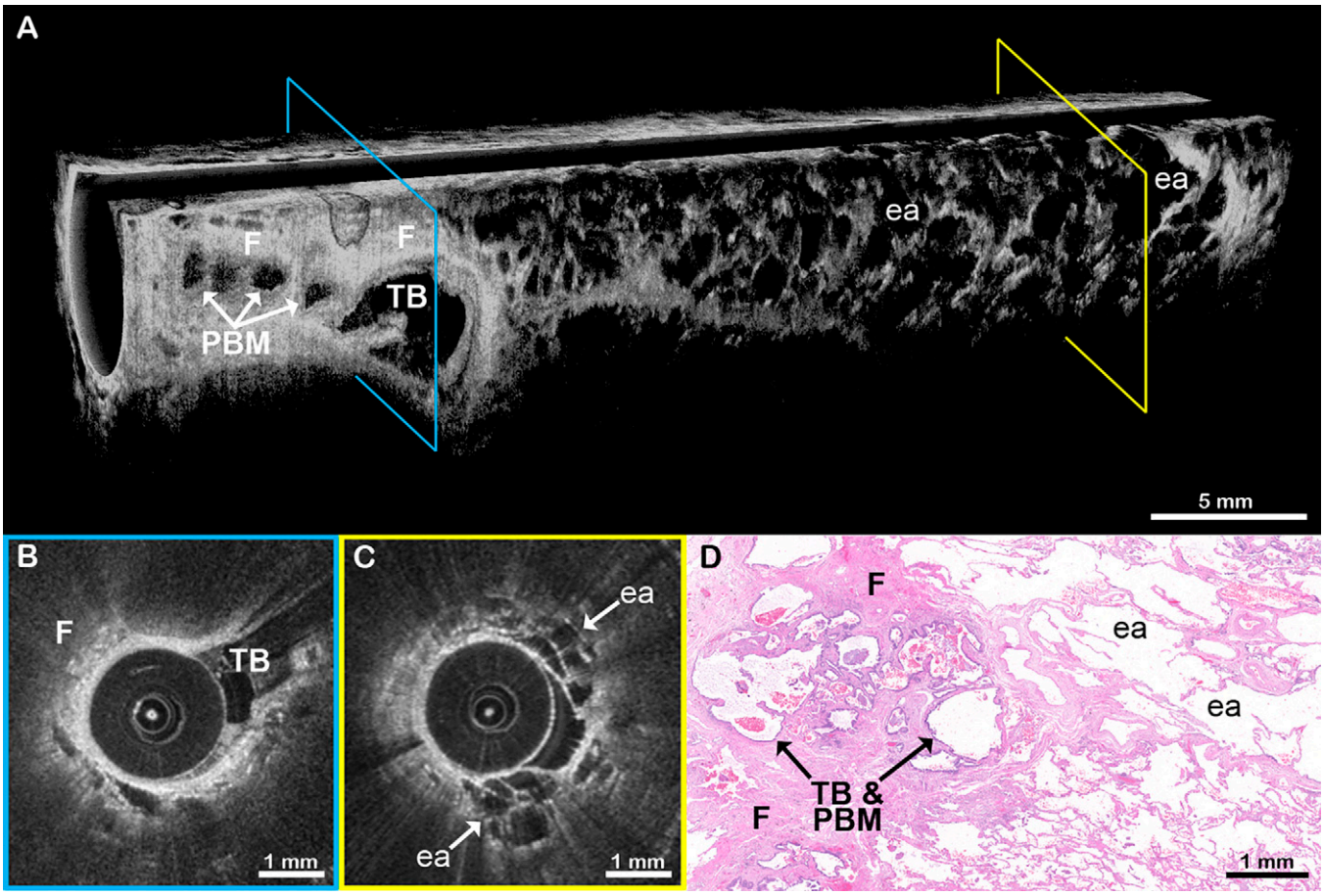

Figure 7. EB-OCT in a patient with airway-centered fibrosis. (*A*) *In vivo* volumetric and (*B* and *C*) cross-sectional EB-OCT from the lower lobe of a patient shows dense, signal-intense fibrosis surrounding the proximal end of the airway (left side). Traction bronchiectasis within the fibrotic region appears as a cystically dilated, irregular airway branch point. Adjacent, smaller, irregular cystic structures are indicative of peribronchiolar metaplasia, often associated with traction bronchiectasis in airway-centered fibrosis. Distal to the airway-centered fibrosis, there is a transition to alveolated parenchyma with enlarged, rounded airspaces and intact alveolar walls, indicative of hyperinflation. (*D*) Surgical lung biopsy confirmed the diagnosis of airway-centered fibrosis with traction bronchiectasis, peribronchiolar metaplasia, and enlarged airspaces with intact alveolar walls. The EB-OCT cross-sections in *B* and *C* are taken from the locations on the volumetric image (*A*) indicated by the blue and yellow squares, respectively. ea = enlarged, rounded airspaces; EB-OCT = endobronchial optical coherence tomography; F = fibrosis; PBM = peribronchiolar metaplasia; TB = traction bronchiectasis.

without OCT experience can be trained to interpret OCT imaging in lung cancer, with a sensitivity and specificity >90% (23). In future studies, we plan to train bronchoscopists to assess EB-OCT data for adequacy.

ILD is notoriously heterogeneous (2, 3, 35). Owing to the large sampling volume and number of sites imaged, EB-OCT is potentially less likely to suffer from the sampling error that occurs in SLB and TBLC. We navigated to and conducted EB-OCT in diseased regions in all lung lobes without difficulty, including assessing multiple locations within the same lobe and across multiple lobes in both lungs, neither of which can be done easily with SLB or TBLC. In 25 patients, we collected four to nine EB-OCT imaging sites per patient. In two cases, we demonstrated sampling superior to the concurrent lung biopsy sample. In one patient, EB-OCT detected UIP features including microscopic honeycombing, whereas the SLB result was more ambiguous, leading to a consensus diagnosis of UIP but with varying opinions among the reviewing pathologists. The diagnosis of UIP was ultimately confirmed 3 years later, on surgical explant lung histology at the time of lung transplantation. In a second case, UIP was diagnosed by EB-OCT when the concurrent TBLC specimen was nondiagnostic. A subsequent SLB later confirmed the diagnosis of UIP. IPF was diagnosed in both patients on clinical follow-up.

Despite the relatively small sample size, this study was adequately powered to assess the sensitivity and specificity of EB-OCT for the diagnosis of UIP on SLB and IPF on clinical follow-up (34). We demonstrated high agreement (weighted $\kappa = 0.87$) between EB-OCT and SLB for the diagnosis of microscopic fibrotic ILD pattern, which is a critical element in MDD for ILD diagnosis. However, we did not have a sufficient sample size to assess the accuracy of diagnosing specific non-

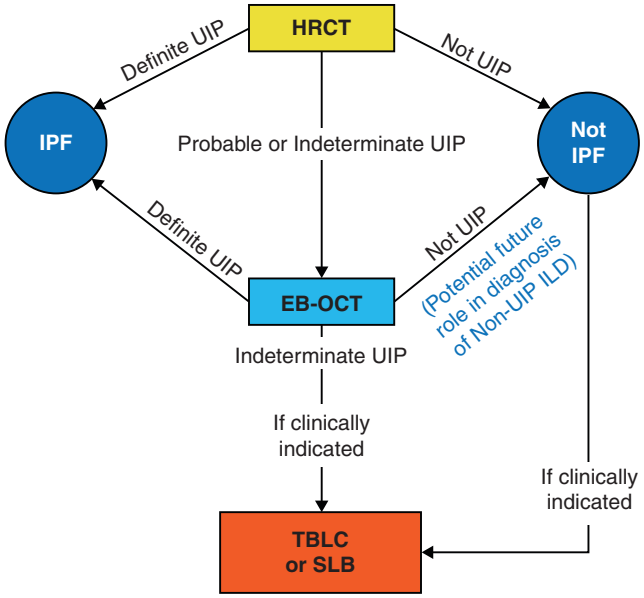

Figure 8. Flow diagram of potential incorporation of EB-OCT in clinical ILD diagnostic workflow. EB-OCT = endobronchial optical coherence tomography; HRCT = high-resolution computed tomography; ILD = interstitial lung disease; IPF = idiopathic pulmonary fibrosis; SLB = surgical lung biopsy; TBLC = transbronchial lung cryobiopsy; UIP = usual interstitial pneumonia.

UIP/IPF ILD entities, such as FHP or CTD-ILD cases. We will investigate this in future, larger-scale, multicenter studies.

EB-OCT could be combined with TBLC for targeted tissue sampling based on EB-OCT–detected abnormality. An illustrative example from our cohort is the case of diffuse idiopathic pulmonary neuroendocrine cell hyperplasia with carcinoid tumorlets diagnosed on SLB. EB-OCT in this patient showed mild ACF with hyperinflation and a small, mass-like lesion within the airway, which, in retrospect, was likely a carcinoid tumorlet. Although EB-OCT alone could not identify the small airway lesion as a carcinoid tumorlet, pairing it with TBLC could allow for targeted sampling of the mass and airway narrowing for diagnosis. Similarly, combining EB-OCT with genomic classifiers may also provide additional diagnostic information (18). In future studies, we aim to investigate EB-OCT with guided TBLC sampling for ILD diagnosis.

Although MDD is generally considered the gold standard for ILD diagnosis, our aim was to evaluate EB-OCT as a possible alternative to SLB (2, 3). Accordingly, we selected our primary comparator to be SLB diagnosis. Given the novelty of EB-OCT at this time, MDDs could not be reasonably expected to appropriately integrate EB-OCT into their assessment. In lieu of MDD, we compared EB-OCT diagnosis against independent clinical follow-up diagnosis from the patients' treating pulmonologists, the majority of which were presented at MDD conference. Similarly, an adaptation of EB-OCT to the 2018 ATS and Fleischner Society guideline histopathology categories (Probable UIP, Indeterminate for UIP, and Alternative Diagnosis) (2, 3) would have been challenging because of the novelty of the modality. In future studies, we will create a training data set from the results of this study to train MDD participants and test with a separate validation data set to compare the impact of EB-OCT with that of SLB in MDD assessment of ILD. We will also adapt the 2018 ATS and Fleischner Society UIP categorization for EB-OCT assessment (2, 3).

There were some limitations to our study. A minor OCT system malfunction immediately before bronchoscopy/SLB prohibited the collection of EB-OCT data in one patient, while an EB-OCT catheter malfunction during the imaging procedure limited the amount of data collected in a second patient. These events are rare and are unlikely to be recurring issues, as demonstrated by successful EB-OCT imaging in the remaining cases. Although the study was limited to a single site, the patients enrolled were referred for lung biopsy by six different treating pulmonologists, which reduces potential practice bias from any single provider. Furthermore, we successfully trained nine bronchoscopists and three pathologists, all with little to no prior OCT experience, to obtain adequate EB-OCT imaging data with no adverse events and to interpret EB-OCT imaging data with high sensitivity and specificity for UIP. We anticipate that we would achieve similar results when training bronchoscopists and pathologists at other institutions. However, future multicenter studies will need to be performed to confirm that the findings in this study can be replicated at other institutions.

Given its low-risk nature, other potential uses of EB-OCT may be explored in the future for research and/or clinical purposes. Repeat, longitudinal EB-OCT imaging may be useful to assess disease progression over time, either to study natural history of disease development in untreated patients or to study therapeutic response in patients using therapy. EB-OCT may also have utility in assessing asymptomatic patients with interstitial lung abnormalities on HRCT as a method of identifying microscopic features of progressive fibrosis and could therefore

potentially identify which patients may benefit from early therapeutic intervention.

Conclusions

This study provides evidence supporting the utility of EB-OCT as a safe, low-risk method for the microscopic diagnosis of ILD, particularly for the diagnosis of histopathologic UIP and clinical IPF. The findings in this study support the use of EB-OCT as a potential future part of ILD diagnostic work-up (Figure 8), as a complement to HRCT and an alternative to SLB. Additional, larger-scale multicenter studies will need to be performed to confirm that the findings of this study can be replicated at other institutions and to further evaluate the role of EB-OCT for the diagnosis of non-UIP ILDs. ■

Author disclosures are available with the text of this article at www.atsjournals.org.

Acknowledgment: The authors thank Susan Sheng, Ph.D., from the Division of Pulmonary and Critical Care Medicine at Massachusetts General Hospital for helping with review and revision of the manuscript. The author(s) meet criteria for authorship as recommended by the International Committee of Medical Journal Editors.

References

1. Daniil ZD, Gilchrist FC, Nicholson AG, Hansell DM, Harris J, Colby TV, *et al.* A histologic pattern of nonspecific interstitial pneumonia is associated with a better prognosis than usual interstitial pneumonia in patients with cryptogenic fibrosing alveolitis. *Am J Respir Crit Care Med* 1999;160:899–905.
2. Raghu G, Remy-Jardin M, Myers JL, Richeldi L, Ryerson CJ, Lederer DJ, *et al.*; American Thoracic Society, European Respiratory Society, Japanese Respiratory Society, and Latin American Thoracic Society. Diagnosis of idiopathic pulmonary fibrosis: an official ATS/ERS/JRS/ALAT clinical practice guideline. *Am J Respir Crit Care Med* 2018;198: e44–e68.
3. Lynch DA, Sverzellati N, Travis WD, Brown KK, Colby TV, Galvin JR, *et al.* Diagnostic criteria for idiopathic pulmonary fibrosis: a Fleischner Society white paper. *Lancet Respir Med* 2018;6:138–153.
4. King TE Jr, Bradford WZ, Castro-Bernardini S, Fagan EA, Glaspole I, Glassberg MK, *et al.*; ASCEND Study Group. A phase 3 trial of pirfenidone in patients with idiopathic pulmonary fibrosis. *N Engl J Med* 2014;370:2083–2092.
5. Richeldi L, du Bois RM, Raghu G, Azuma A, Brown KK, Costabel U, *et al.*; INPULSIS Trial Investigators. Efficacy and safety of nintedanib in idiopathic pulmonary fibrosis. *N Engl J Med* 2014;370:2071–2082.
6. Flaherty KR, Wells AU, Cottin V, Devaraj A, Walsh SLF, Inoue Y, *et al.*; INBUILD Trial Investigators. Nintedanib in progressive fibrosing interstitial lung diseases. *N Engl J Med* 2019;381:1718–1727.
7. Albera C, Costabel U, Fagan EA, Glassberg MK, Gorina E, Lancaster L, *et al.* Efficacy of pirfenidone in patients with idiopathic pulmonary fibrosis with more preserved lung function. *Eur Respir J* 2016;48:843–851.
8. Costabel U, Inoue Y, Richeldi L, Collard HR, Tschoepe I, Stowasser S, *et al.* Efficacy of nintedanib in idiopathic pulmonary fibrosis across prespecified subgroups in INPULSIS. *Am J Respir Crit Care Med* 2016; 193:178–185.
9. Idiopathic Pulmonary Fibrosis Clinical Research Network; Raghu G, Anstrom KJ, King TE, Lasky JA, Martinez FJ. Prednisone, azathioprine, and N-acetylcysteine for pulmonary fibrosis. *N Engl J Med* 2012;366: 1968–1977.
10. Brownell R, Moua T, Henry TS, Elicker BM, White D, Vittinghoff E, *et al.* The use of pretest probability increases the value of high-resolution CT in diagnosing usual interstitial pneumonia. *Thorax* 2017;72:424–429.
11. Chung JH, Chawla A, Peljto AL, Cool CD, Groshong SD, Talbert JL, *et al.* CT scan findings of probable usual interstitial pneumonitis have a high predictive value for histologic usual interstitial pneumonitis. *Chest* 2015; 147:450–459.
12. Raghu G, Lynch D, Godwin JD, Webb R, Colby TV, Leslie KO, *et al.* Diagnosis of idiopathic pulmonary fibrosis with high-resolution CT in patients with little or no radiological evidence of honeycombing: secondary analysis of a randomised, controlled trial. *Lancet Respir Med* 2014; 2:277–284.
13. Raghu G, Mageto YN, Lockhart D, Schmidt RA, Wood DE, Godwin JD. The accuracy of the clinical diagnosis of new-onset idiopathic pulmonary fibrosis and other interstitial lung disease: a prospective study. *Chest* 1999;116:1168–1174.
14. Iftikhar IH, Alghothani L, Sardi A, Berkowitz D, Musani AI. Transbronchial lung cryobiopsy and video-assisted thoracoscopic lung biopsy in the diagnosis of diffuse parenchymal lung disease: a meta-analysis of diagnostic test accuracy. *Ann Am Thorac Soc* 2017;14:1197–1211.
15. Hutchinson JP, Fogarty AW, McKeever TM, Hubbard RB. In-hospital mortality after surgical lung biopsy for interstitial lung disease in the United States. 2000 to 2011. *Am J Respir Crit Care Med* 2016;193: 1161–1167.
16. Romagnoli M, Colby TV, Berthet J-P, Gamez AS, Mallet J-P, Serre I, *et al.* Poor concordance between sequential transbronchial lung cryobiopsy and surgical lung biopsy in the diagnosis of diffuse interstitial lung diseases. *Am J Respir Crit Care Med* 2019;199:1249–1256.
17. Troy LK, Grainge C, Corte TJ, Williamson JP, Vallely MP, Cooper WA, *et al.*; Cryobiopsy versus Open Lung biopsy in the Diagnosis of Interstitial lung disease alliance (COLDICE) Investigators. Diagnostic accuracy of transbronchial lung cryobiopsy for interstitial lung disease diagnosis (COLDICE): a prospective, comparative study. *Lancet Respir Med* 2020;8:171–181.
18. Raghu G, Flaherty KR, Lederer DJ, Lynch DA, Colby TV, Myers JL, *et al.* Use of a molecular classifier to identify usual interstitial pneumonia in conventional transbronchial lung biopsy samples: a prospective validation study. *Lancet Respir Med* 2019;7:487–496.
19. Yun SH, Tearney GJ, Vakoc BJ, Shishkov M, Oh WY, Desjardins AE, *et al.* Comprehensive volumetric optical microscopy in vivo. *Nat Med* 2006;12:1429–1433.
20. Hariri LP, Adams DC, Wain JC, Lanuti M, Muniappan A, Sharma A, *et al.* Endobronchial optical coherence tomography for low-risk microscopic assessment and diagnosis of idiopathic pulmonary fibrosis in vivo. *Am J Respir Crit Care Med* 2018;197:949–952.
21. Yun S, Tearney G, Bouma B, Park B, de Boer J. High-speed spectral-domain optical coherence tomography at 1.3 mum wavelength. *Opt Express* 2003;11:3598–3604.
22. Adams DC, Miller AJ, Applegate MB, Cho JL, Hamilos DL, Chee A, *et al.* Quantitative assessment of airway remodelling and response to allergen in asthma. *Respirology* 2019;24:1073–1080.
23. Hariri LP, Mino-Kenudson M, Applegate MB, Mark EJ, Tearney GJ, Lanuti M, *et al.* Toward the guidance of transbronchial biopsy: identifying pulmonary nodules with optical coherence tomography. *Chest* 2013;144:1261–1268.
24. Hariri LP, Adams DC, Applegate MB, Miller AJ, Roop BW, Villiger M, *et al.* Distinguishing tumor from associated fibrosis to increase diagnostic biopsy yield with polarization-sensitive optical coherence tomography. *Clin Cancer Res* 2019;25:5242–5249.
25. Hariri LP, Applegate MB, Mino-Kenudson M, Mark EJ, Medoff BD, Luster AD, *et al.* Volumetric optical frequency domain imaging of pulmonary pathology with precise correlation to histopathology. *Chest* 2013;143: 64–74.
26. Raphaely RA, Nandy S, Muniappan A, Shih A, Roop B, Sharma A, *et al.* Endobronchial optical coherence tomography: a novel method for the microscopic diagnosis of usual interstitial pneumonia and idiopathic pulmonary fibrosis [abstract]. *Am J Respir Crit Care Med* 2021;A1853.
27. Hariri LP, Nandy S, Roop BW, Adams DC, Muniappan A, Keyes C, *et al.* Endobronchial optical coherence tomography for in vivo microscopic diagnosis of pulmonary fibrosis [abstract]. *Am J Respir Crit Care Med* 2020;201:A2562.

28. Hariri LP, Adams DC, Roop BW, Muniappan A, Keyes C, Wain JC, *et al.* Polarization sensitive optical coherence tomography for in vivo microscopic detection of pulmonary fibrosis [abstract]. *Am J Respir Crit Care Med* 2019;199:A4321.
29. Hariri LP, Adams DC, Wain JC, Lanuti M, Muniappan A, Sharma A, *et al.* Endobronchial optical coherence tomography for in vivo microscopic assessment and diagnosis of idiopathic pulmonary fibrosis [abstract]. *Am J Respir Crit Care Med* 2018;197:A1103.
30. Nandy S, Israel RA, Muniappan A, Shih A, Roop BW, Sharma A, *et al. In vivo* microscopic assessment of idiopathic pulmonary fibrosis using endobronchial optical coherence tomography: a prospective diagnostic study. Oral presentation at The Optical Coherence Tomography and Coherence Domain Optical Methods in Biomedicine XXV. SPIE Photonics West. March 2021, Virtual.
31. Hariri LP, Nandy S, Roop BW, Adams DC, Muniappan A, Keyes CK, *et al.* Endobronchial optical coherence tomography for *in vivo* microscopic diagnosis of pulmonary fibrosis. Optical Coherence Tomography and Coherence. Oral presentation at The Optical Methods in Biomedicine XXIV. SPIE Photonics West. February 2020, San Francisco, CA.
32. Raphaely R, Nandy S, Muniappan A, Shih A, Roop BW, Sharma A, *et al.* Endobronchial optical coherence tomography accurately diagnoses microscopic usual interstitial pneumonitis and clinical idiopathic pulmonary fibrosis. Poster presentation at The National Jewish Health 17th Annual Respiratory Disease Young Investigators' Forum. October 2020, Virtual.
33. Raghu G, Collard HR, Egan JJ, Martinez FJ, Behr J, Brown KK, *et al.*; ATS/ERS/JRS/ALAT Committee on Idiopathic Pulmonary Fibrosis. An official ATS/ERS/JRS/ALAT statement: idiopathic pulmonary fibrosis: evidence-based guidelines for diagnosis and management. *Am J Respir Crit Care Med* 2011;183:788–824.
34. Flahault A, Cadilhac M, Thomas G. Sample size calculation should be performed for design accuracy in diagnostic test studies. *J Clin Epidemiol* 2005;58:859–862.
35. Leslie KO. My approach to interstitial lung disease using clinical, radiological and histopathological patterns. *J Clin Pathol* 2009;62:387–401.